JCTC Journal of Chemical Theory and Computation

ARTICLE

pubs.acs.org/JCTC

Intra- and Interatomic Spin Interactions by the Density Functional Theory plus *U* Approach: A Critical Assessment

Yachao Zhang and Hong Jiang*

Beijing National Laboratory of Molecular Sciences, State Key Laboratory of Rare Earth Materials Chemistry and Applications, College of Chemistry and Molecular Engineering, Peking University, Beijing, 100871, China

Supporting Information

ABSTRACT: Accurate evaluation of the total energy difference between different spin states in molecular magnetic systems is currently a great challenge in theoretical chemistry. In this work we assess the performance of the density functional theory plus the Hubbard *U* (DFT+*U*) approach for the first-principles description of the high spin-low spin (HS-LS) splitting and the exchange coupling constant, corresponding to the intra- and interatomic spin interactions, respectively. The former is investigated using a set of mononuclear ion complexes with different HS-LS splitting, including seven spin-crossover (SCO) compounds, while the latter is investigated in a series of binuclear copper complexes covering both ferromagnetic and antiferromagnetic interactions. We find that the DFT+*U* approach can reproduce experimental data as accurately as the hybrid functionals approach but with much lower computational efforts. We further analyze the effect of *U* in terms of spin density on magnetic centers, and we find that the main effect of the *U* correction can be attributed to the enhanced localization of magnetic orbitals. Even taking the uncertainty related to the determination of *U* into account, we think the DFT+*U* approach is an efficient and predictive first-principles method for the SCO phenomenon and interatomic magnetic interactions.

1. INTRODUCTION

Recent years have seen a remarkable revival of interest in molecular magnetism[1,2] due to the unique role it plays in molecule-based spintronics.[3,4] By exploiting electronic charge and spin degrees of freedom simultaneously at the molecular level, molecular spintronics holds great hope on a wide range of applications, such as molecule-based memory,[5] switches,[6] and quantum computation.[7,8] A large number of molecular magnetic systems have been discovered and brought under intensive investigation. Among them two kinds of materials, spin-crossover (SCO)[9] compounds and single-molecule magnets (SMMs),[10] are of particular interest. Their unique magnetic bistable states and spin transition (reversal) behavior make them promising candidates for data storage materials, switching devices, displays, and sensors.[5,6,11,12] A SCO compound is one in which an intra-atomic, reversible low spin-high spin (LS-HS) transition, often occurring in octahedral coordinated d^4–^{7} transition-metal complexes, can be readily induced by a variety of external stimuli, such as temperature, pressure, and light irradiation. The necessary condition for the spin transition to occur is that the perturbation energy is approximately equal to the energy splitting between the LS and the HS states:

$$\Delta E_{\text{H-L}} \equiv E_{\text{HS}} - E_{\text{LS}} \tag{1}$$

The energy splitting $\Delta E_{\text{H-L}}$ largely determines the critical parameter characterizing the transition, such as the spin transition temperature (T_c).[9,13] Physically $\Delta E_{\text{H-L}}$ is mainly determined by the two competing factors, the effective electron-pairing energy (P) of the d electrons and the crystal-field splitting (Δ_o), which, when dominant, favors HS and LS ground states, respectively.[14] The magnitude of $\Delta E_{\text{H-L}}$ in typical SCO compounds is usually quite small, falling in the range of 0–0.3 eV (i.e., 0–30 kJ/mol).[13] An accurate evaluation of this quantity is therefore highly challenging from a theoretical point of view. While the SCO phenomenon is mainly determined by the intra-atomic spin coupling, a SMM is characterized by a strong interatomic spin interaction, which gives rise to a large collective ground-state spin (S). When the large spin is combined with a large magnetic anisotropy as a result of the spin–orbit coupling (SOC), the spin-reversal process between spin-up and spin-down configurations will be blocked by an energy barrier DS^2 (D, axial zero-field splitting parameter), which eventually determines the blocking temperature (T_B).[10,15] A room-temperature T_B is required for a SMM system to be practically useful, for which a large S and/or a large D are needed. Large ground-state spins can be formed from strong collective interactions among local magnetic moments in polynuclear molecular clusters (e.g., $Mn_{12}O_{12}$).[10] The interatomic spin–spin interaction is usually described by a phenomenological Heisenberg Hamiltonian:[16]

$$\hat{H} = -J\hat{S}_i \cdot \hat{S}_j \tag{2}$$

Here $\hat{S}_i$ and $\hat{S}_j$ represent the spin operators of the coupling magnetic centers i and j, respectively, and J is the intersite exchange coupling constant that characterizes the type [positive J, ferromagnetic (FM); negative J, antiferromagnetic (AFM)] and the strength of the magnetic interactions between neighboring magnetic centers. Compared to S, it is even more challenging to attain a large D, which depends on both strong spin–orbit coupling and constructive alignment of individual anisotropy axes on different magnetic centers. To make things

Received: May 2, 2011
Published: August 01, 2011

more complicated, there is clear evidence from both theory and experiment that the total magnetic anisotropy of a polynuclear cluster can often be dramatically reduced as a result of mutual cancellation of the local anisotropies so that a large ground-state spin S is often accompanied by a very small zero-field splitting.[17]

Accurate evaluation of the two key parameters, $\Delta E_{\text{H-L}}$ and J, is currently a great challenge in theoretical chemistry. Both quantities are determined by the energy difference between different spin configurations of open-shell (i.e., with unpaired electrons) systems, for which theoretical chemistry is much less well developed than that of closed-shell systems. For open-shell systems, the electronic ground state in general cannot be described based on the single Slater determinant-based approaches, like Hartree−Fock (HF) or Kohn−Sham (KS) density functional theory (DFT). A theoretically rigorous treatment of them requires using correlated wave function-based approaches, such as the multireference perturbation theory (e.g., CASPT2), configuration interaction (MRCI), or coupled cluster (MRCC) methods.[18−22] They are, however, too expensive to be applied routinely for practically interesting molecular magnetic systems with tens or even hundreds of atoms. It is even more difficult to apply the correlated wave function-based approaches to crystalline systems, the form in which molecular magnetic systems are usually studied experimentally. Currently most first-principles studies of molecular magnetic systems are based on HF or KS DFT. As a result of their single-determinant framework, additional approximations are often needed to relate theoretically calculated quantities to $\Delta E_{\text{H-L}}$ and J.

Although sharing a similar single-configuration framework, HF and DFT exhibit very different performances in terms of their descriptions of magnetic properties, owing to their different treatment of the exchange−correlation (xc) interaction. Due to the lack of dynamic Coulomb correlation, electrons in HF tend to get too close to each other so that the electron-pairing energy (denoted as P henceforth) is often overestimated. Therefore, HF favors the HS ground state.[13] On the other hand, KS DFT in the local density or generalized gradient approximation (LDA or GGA, respectively) to the xc energy functionals suffers from the self-interaction error (SIE) problem.[23] As a result, electrons tend to repel each other artificially, leading to a tendency to stabilize the LS state,[24,25] and the local magnetic orbitals (singly occupied molecular orbitals) are delocalized, thus overestimating the magnetic interactions.[26] The SIE problem of LDA or GGA can be partially remedied by mixing a fraction of the HF (exact) exchange with the standard LDA or GGA xc functionals,[27,28] hence termed the hybrid functionals approach, which has become the most successful DFT method for molecular systems.[29] The hybrid functionals approach has also been applied to molecular magnetic systems recently, and the overall performance is very promising.[30−32] It has, however, at least two drawbacks. The results often depend quite sensitively on the parameters used in these functionals, including in particular the percentage of the exact exchange that is included. Different materials (or properties) need different parameters to obtain optimal results.[30−32] From a practical point of view, the hybrid functionals approach, when implemented with the periodic boundary condition that is used in most popular first-principles DFT packages, is computationally much more expensive than standard LDA or GGA. Therefore, although the hybrid functionals approach has become popular in computational chemistry since two decades ago,[29] its use in computational materials science is much more limited, and it becomes available in popular DFT packages only very recently.[33,34]

For systems with partially occupied d- or f-states, a simple and effective approach that can overcome the major failure of LDA or GGA is to introduce a local correction characterized by the Hubbard Coulomb interaction term U,[35] hence termed LDA (GGA)+U (or more generally DFT+U).[36−38] Physically the U correction has the effect of introducing a penalty for fractional occupation that is favored by LDA or GGA. DFT+U was originally developed to describe Mott insulators[39] properly in the band theory framework and has become a popular first-principles method for strongly correlated materials during the past decade.[40] Only recently have a few attempts been made to apply the approach in molecular magnetic systems.[41−45] It was found that the DFT+U method can in general improve the description of magnetic interactions considerably, but its overall performance is still inconclusive.[41−45] Rivero et al.[44] applied the plane wave-based DFT+U approach to investigate magnetic coupling constants of a series of binuclear copper complexes. They showed that the description of AFM systems was significantly improved by DFT+U but that of FM ones was still quite poor.

The main goal of this work is to investigate the performance of the DFT+U method for the evaluation of $\Delta E_{\text{H-L}}$ and J in a systematic manner. For $\Delta E_{\text{H-L}}$, we consider a set of mononuclear iron complexes including seven SCO compounds. For J, we study a group of binuclear copper complexes that cover both FM and AFM intersite interactions. The paper is organized as follows. In the next section, Section 2, we present the method used in our investigation and some computational details. In Section 3, we first show that the DFT+U method is able to describe the SCO phenomenon and exchange interactions with an accuracy that is comparable to the state-of-the-art hybrid functionals approaches. Then the physical effect of U is analyzed in terms of the variation of local spin density projected on magnetic centers, from which we argue that the Hubbard U correction can effectively induce localization of magnetic orbitals to eliminate their erroneous overlap with other orbitals. In Section 4 we conclude the work with a few general remarks regarding the limitation of the DFT+U approach for molecular magnetic systems.

2. COMPUTATIONAL DETAILS

To investigate the performance of DFT+U for the description of intra-atomic spin interaction, we consider seven iron(II) complexes[46−50] with different ground spin states and seven iron SCO compounds[51−64] for which experimental data for the enthalpy difference ΔH between different spin states (iron(II): LS, $S = 0$; HS, $S = 2$ and iron(III): LS, $S = 1/2$; HS, $S = 5/2$) are available. We calculate $\Delta E_{\text{H-L}}$ in terms of eq 1, where the total energies in the HS and LS states are obtained from standard spin-unrestricted KS DFT calculations with fully optimized molecular structures.

For the calculation of J that characterizes the interatomic spin coupling, we use the "broken symmetry" (BS) approach:[65,66] J is related to the total energy difference between the HS state, in which the neighboring magnetic ions have parallel spin alignment ($\uparrow\uparrow$) and a constructed BS state with the corresponding antiparallel spin alignment ($\uparrow\downarrow$). By assuming fully localized magnetic orbitals and using the Heisenberg Hamiltonian (eq 2),[66] one obtains

$$E_{\text{BS}} - E_{\text{HS}} = \langle\uparrow\downarrow| - J\hat{S}_i\cdot\hat{S}_j|\uparrow\downarrow\rangle - \langle\uparrow\uparrow| - J\hat{S}_i\cdot\hat{S}_j|\uparrow\uparrow\rangle = 2JS_iS_j \quad (3)$$

where S_i and S_j are the spin quantum numbers of the two interacting local magnetic centers. We consider only binuclear

copper(II) complexes,[67−77] which have $S_i = S_j = 1/2$, so that the exchange coupling constant can be calculated by

$$J = 2(E_{BS} - E_{HS}) \quad (4)$$

We use the molecular structures extracted from the crystal data without further structural optimization, which is a common practice in the studies of exchange coupling constants to avoid additional uncertainty.[26]

All calculations are performed using the SIESTA code[78,79] (with the DFT+U extension[80]), which is based on numerical atomic basis[78] and norm-conserving pseudopotentials (NCPPs).[81] The capability of the code to treat molecular magnetic systems has been well verified by Ruiz et al.[82] We use the triple-ζ plus polarization (TZP) basis for magnetic ions (Fe, Cu), and the double-ζ plus polarization (DZP) basis for the other atoms. Both LDA[23] and Perdew−Burke−Erzernhof (PBE)[83] GGA functionals are used in our calculations.

The DFT+U calculations are based on the simplified rotationally invariant scheme by Dudarev et al.[37] in which the parameter U corresponds to $U-J$ in the original formulas proposed by Anisimov et al.,[36] with J here being the onsite exchange interaction. Considering the important role of U, a few comments on the choice of U are in order. U is defined physically as the effective on-site Coulomb interaction among localized electrons in partially occupied d- or f-shells, which is determined mainly by the nature of localized d or f electrons and their chemical environments. The Hubbard U correction is introduced in DFT+U mainly to overcome the severe SIE among localized d or f electrons. In practice, however, U is often regarded as an adjustable parameter, whose value is determined by fitting to experiment. This is in some sense to use U to correct not only SIE but also all other errors of a particular LDA or GGA functional. Such empiricism in the DFT+U approach is certainly useful to greatly enhance its applicability to a wide range of complicated materials for which more accurate and theoretically more rigorous methods are infeasible. On the other hand, the predictive power of DFT+U can be impaired, and more importantly, the physical significance of U can be lost if the adjustability of U is overused. Using different target properties for fitting may result in significantly different values of U, and the situation can become more complicated if the experimental data used for fitting have significant uncertainty (error bar). Therefore, we think U should be chosen based on physical considerations, either by fitting to the experimental data that carry the information of on-site Coulomb interaction, such as photoemission spectroscopic (PES) data,[84,85] or calculated from first-principles approaches, such as the constrained DFT.[38,86−88] Although a unique determination of U is difficult, a physical range of U can be easily established for a particular transition-metal ion. Guided by these considerations, we use in this work U = 4.0 eV for Fe(II) and Fe(III) and U = 6.5 eV for Cu(II) based on previous constrained DFT calculations and PES experimental data for some simple Fe(II)[38,85,88] and Cu(II)[85,89] inorganic materials. Rigorously speaking, the value of U should depend on the oxidation state and the chemical environments of the transition-metal ion, which are, however, secondary factors. We leave further investigation of this issue to the future. Finally we note that although the dependence on U introduces uncertainty when interpreting the results from DFT+U, we can also take advantage of such dependence in the spirit of a Gendanken experiment; since U characterizes the strength of onsite Coulomb interaction, we can obtain insights on physical mechanisms underlying different spin interactions by investigating how physical properties under study depend on the value of U.

Table 1. Assessment of the Pseudopotentials and Basis Used in This Work by Comparing the Calculated $\Delta E_{H\text{-}L}$ (kJ/mol)[a] of $[Fe(2\text{-}A)_3]^{2+}$ with That Obtained Using ECP and All-Electron Basis

basis[b]	TZP	Lanl2dz	6-311+G(d)
LDA	544	533	552
GGA	447	428	450

[a] Structures determined at 12 and 298 K are used as in LS and HS states, respectively. [b] Different basis sets are employed for iron: TZP in SIESTA (DZP for the other atoms) and Lanl2dz and 6-311+G(d) in GAUSSIAN09 (6-31G(d) for the others).

We use the NCPPs taken from ABINIT's pseudopotential database,[90] as provided by the SIESTA group,[80] for all elements involved in our calculations except for iron. For the latter, a NCPP with nonlinear core correction (NLCC)[81] is generated based on the nonrelativistic spin-polarized atomic calculations ($[Ar]3d^64s^2$) with a cutoff radius of 2.0 Bohr for all the angular components. The inclusion of NLCC in the pseudopotential is found to be crucial for the accurate description of the Fe 3d states.

To check the accuracy of the pseudopotentials as well as the numerical atomic basis functions used in our calculations, we compare $\Delta E_{H\text{-}L}$ of $[Fe(2\text{-}A)_3]^{2+}$ (2-A = 2-picolylamine)[58] calculated by SIESTA with that by GAUSSIAN09[91] using both all-electron and effective core potential (ECP) basis (see Table 1). The results from SIESTA are in excellent agreement with all-electron and small-core ECP results, which confirms the accuracy of the method used in our calculations.

3. RESULTS AND DISCUSSION

3.1. Spin-Crossover of Iron Complexes. We begin the analysis by inspecting a series of iron(II) complexes with significantly different ground-state spin properties (Table 2). This list of compounds is ordered in terms of the magnitude of Δ_o that is determined by the coordination nature of the ligands. Since $\Delta E_{H\text{-}L}$ depends on Δ_o linearly, the results are expected to change from large positive values for the compounds coordinated with NO^+ and CO to negative ones for those with NH_3 and H_2O. This trend is indeed well delivered by all theoretical methods except GGA+U, which overstabilizes the HS state dramatically such that it completely loses the ability to distinguish between HS and LS states. We note that GGA+U with a significantly smaller U (∼ 1.0 eV) would give much improved results, but using such a small U is physically not well founded. A more quantitative assessment is however not straightforward, since the only experimental information available is the nature (HS or LS) of the ground state, i.e., the sign of $\Delta E_{H\text{-}L}$. We will therefore take the results obtained from CASPT2[18] as the benchmark. In general, GGA yields quite accurate results, but its performance is not systematic. In particular, for $[Fe(N_2H_4)(NHS_4)]$ and $[Fe(NH_3)(NHS_4)]$ (NHS_4^{2-} = 2,2′-bis(2-mercaptophenylthio)),[49] $\Delta E_{H\text{-}L}$ calculated by GGA is about ten times larger than that by CASPT2. Compared to GGA, LDA tends to favor the LS states more strongly, and therefore, $\Delta E_{H\text{-}L}$ is significantly overestimated. Overall the best performance is obtained by LDA+U, which gives results closely comparable with those from the

Table 2. Calculated $\Delta E_{H\text{-}L}$ (kJ/mol) Compared with Results Obtained by TPSSh and CASPT2

compound	LDA	LDA+U	GGA	GGA+U	TPSSh[a]	CASPT2[b]	expt[c]	ref
$[Fe^{II}(NO^{+})(NHS_4)]$[d]	204	71	123	−42	102	178	LS	46
$[Fe^{II}(CO)(NHS_4)]$	236	73	139	−35	103	122	LS	47
$[Fe^{II}(PMe_3)(NHS_4)]$	208	36	92	−81	63	81	LS	48
$[Fe^{II}(N_2H_4)(NHS_4)]$	155	3	49	−104	5	4	HS	49
$[Fe^{II}(NH_3)(NHS_4)]$	145	−5	40	−107	−53	5	HS	49
$[Fe^{II}(NH_3)_6]^{2+}$	93	−32	−21	−134	−24	−86	HS	–
$[Fe^{II}(H_2O)_6]^{2+}$	−76	−153	−163	−232	−114	−195	HS	50

[a] Ref 92. [b] Ref 18. [c] Experimental ground spin states: LS, $S = 0$; HS, $S = 2$. [d] NHS_4^{2-} = 2,2′-bis(2-mercaptophenylthio) diethylamine dianion.

Table 3. Calculated $\Delta E_{H\text{-}L}$ (kJ/mol) in Comparison with the Enthalpy Difference ΔH (kJ/mol) Obtained from TPSSh and Experiment

	$\Delta E_{H\text{-}L}$ (kJ/mol)				ΔH (kJ/mol)[a]		
compound	LDA	LDA+U	GGA	GGA+U	TPSSh[b]	expt	ref
$[Fe^{III}(acac)_2trien]^{+}$	126	18	32	−68	33	7−17	51 and 52
$[Fe^{II}(papth)_2]^{2+}$	177	23	51	−95	15	16	53 and 54
$[Fe^{II}(tacn)_2]^{2+}$	141	5	30	−94	16	21−24	55 and 56
$[Fe^{II}(2\text{-}A)_3]^{2+}$	174	20	46	−98	14	18−25	57 and 58
$[Fe^{II}(HB(pz)_3)_2]$	218	47	75	−80	51	16−22	59 and 60
$[Fe^{II}(py(bzimH))_3]^{2+}$	191	28	55	−96	26	20−21	61 and 62
$[Fe^{II}(tppn)]^{2+}$	186	29	58	−88	31	25−30	63 and 64

[a] $\Delta H = \Delta E_{H\text{-}L} + \Delta E_{vib} + p\Delta V$, where the vibrational part ΔE_{vib} contributes to the enthalpy difference a few kJ/mol (negative) but is basically independent of the system; the last term $p\Delta V$ can be ignored. [b] Ref 31.

hybrid functional (TPSSh) approach reported by Ye and Neese.[92]

We further investigate the performance of the DFT+U approach in describing $\Delta E_{H\text{-}L}$ of real SCO complexes. Table 3 shows $\Delta E_{H\text{-}L}$'s of the seven iron SCO compounds obtained from LDA(+U) and GGA(+U), together with the results from TPSSh[31] and the enthalpy differences determined experimentally. Rigorously speaking, ΔH contains, in addition to the electronic energy change $\Delta E_{H\text{-}L}$, the contributions from the change of volume ($p\Delta V$) and the vibrational part (ΔE_{vib}). While the former is expected to be marginal, the latter, mainly the difference in zero-point energies between LS and HS states, is non-negligible because of significantly different metal−ligand (M−L) binding strength in LS and HS states. Nevertheless, the contribution of ΔE_{vib} is typically a few kJ/mol,[31] which is smaller than $\Delta E_{H\text{-}L}$ in typical SCO compounds and comparable to the uncertainty (error bar) in the experimental data of ΔH. Most importantly, ΔE_{vib} is nearly constant for different systems.[25] It is therefore reasonable to compare theoretical results of $\Delta E_{H\text{-}L}$ to experimental ΔH. For these SCO compounds, $\Delta E_{H\text{-}L}$'s from LDA are overestimated dramatically, by nearly 1 order of magnitude. GGA results, however, are only slightly overestimated. The U correction added to GGA again results in qualitatively wrong ground states for all SCO compounds considered. On the other hand, the LDA+U approach gives results very similar to those from TPSSh, both in good agreement with experimental enthalpy differences. We note that for $[Fe(HB(pz)_3)_2]$ ($HB(pz)_3$ = hydro-tris(1-pyrazolyl)-borato),[60] both LDA+U and TPSSh overestimate $\Delta E_{H\text{-}L}$ significantly. On the whole, the LDA+U approach delivers a comparable accuracy as the hybrid functionals approach for the description of the SCO phenomenon.

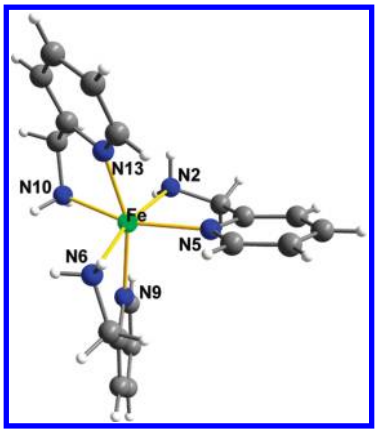

Figure 1. Molecular structure of $[Fe(2\text{-}A)_3]^{2+}$.

Besides an accurate evaluation of $\Delta E_{H\text{-}L}$, a reliable prediction of equilibrium molecular structures in different spin states is also of great importance for the simulation of SCO compounds. To assess the performance of the DFT+U approach for that, we consider $[Fe(2\text{-}A)_3]^{2+}$ (Figure 1), whose experimental crystal structural data in both LS and HS states are available.[58] We note that crystal and finite-temperature effects are not taken into account in our calculations, a common practice in theoretical studies of SCO compounds.[13,31] Optimized M−L bond lengths obtained from different theoretical approaches are compared to experimental ones in Table 4. In the LS state, which is stable at low temperature, the M−L bonds from LDA are systematically shorter than those from experiment, a feature that has been well recognized for transition-metal complexes.[29] LDA+U

Table 4. Experimental and Optimized M−L Bond Lengths (Å) of $[Fe(2\text{-}A)_3]^{2+}$ in the LS and HS States

	LS (S = 0)					HS (S = 2)				
M−L bond	crystal	LDA	LDA+U	GGA	GGA+U	crystal	LDA	LDA+U	GGA	GGA+U
$Fe-N_{10}$	2.024	1.975	2.018	2.030	2.082	2.179	2.220	2.232	2.265	2.303
$Fe-N_{13}$	1.991	1.924	1.975	1.978	2.049	2.196	2.100	2.162	2.191	2.242
$Fe-N_2$	2.020	1.976	2.017	2.033	2.088	2.180	2.218	2.237	2.290	2.280
$Fe-N_5$	2.004	1.936	1.982	2.001	2.061	2.220	2.113	2.164	2.204	2.292
$Fe-N_6$	2.034	1.966	2.011	2.024	2.084	2.183	2.210	2.225	2.250	2.272
$Fe-N_9$	1.998	1.927	1.978	1.990	2.049	2.213	2.097	2.160	2.193	2.258
MAE[a]		0.061	0.015	0.009	0.057		0.071	0.049	0.051	0.079

[a] MAE with respect to the corresponding experimental structures (12 K, LS; 298 K, HS).

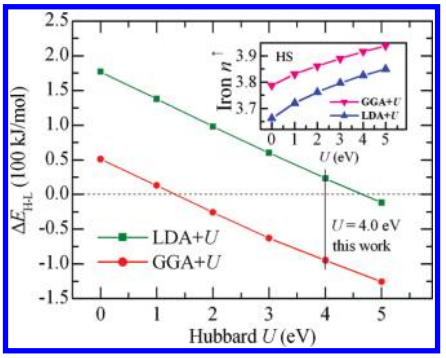

Figure 2. Calculated ΔE_{H-L} of $[Fe(papth)_2]^{2+}$ as a function of U employing LDA+U [green line, solid squares (■)] and GGA+U [red line, solid circles (●)]. Dash line: bottom line of qualitatively correct results. The vertical line refers to the U value used in this work. Inset: spin density $n^{\uparrow}$ of iron (Mulliken population analysis) in HS state versus U [blue line, triangle (▲), LDA+U; pink line, inverse-triangle (▼), GGA+U].

significantly improves the LDA results, reducing the mean absolute error (MAE) from 0.061 to 0.015 Å. On the other hand, since pure GGA already describes M−L bond lengths quite well, the inclusion of the U correction, which tends to increase the M−L bond lengths, results in systematically overestimated bond lengths with a MAE of 0.057 Å with respect to experiment. For the HS state, the overall trend is still similar: LDA+U gives results that are generally in better agreement with experiment than LDA, and GGA+U tends to overestimate the M−L bond lengths systematically. On the other hand, the agreement between theory (LDA+U and GGA) and experiment is noticeably poorer in the HS state than that in the LS state. A likely cause for this is that the experimental data for the HS state are obtained from crystallographic structures measured at room temperature, in contrast to those for the LS state, which is measured at low temperature. We can therefore expect that structural data in the HS state are influenced by crystal and finite-temperature effects more strongly than those in the LS state.

Optimized M−L bond lengths for other SCO compounds considered in this work can be found in the Supporting Information, and they exhibit very similar features. Overall, both PBE-GGA and LDA+U give equilibrium structures with an accuracy comparable to that from BP86-GGA. The latter was shown to give optimal structural properties of transition-metal complexes.[31] Therefore, by using LDA+U, both electronic and structural properties of SCO systems can be described accurately by the same theoretical approach. In contrast, GGA (BP86 or PBE) can only describe structural properties accurately but not electronic properties.

In the following we will take $[Fe(papth)_2]^{2+}$ (papth = 2-(pyridin-2-ylamino)-4-(pyridin-2-yl)thiazole)[54] as an example to analyze how the Hubbard U works. According to the crystal field theory, ΔE_{H-L} can be roughly determined by the difference between the crystal field splitting Δ_o and the mean electron pairing energy P among the localized d electrons,[14] the latter being closely related to the on-site Coulomb repulsion U. This simplified picture is confirmed in Figure 2, which shows that ΔE_{H-L} from LDA+U and GGA+U both decrease linearly as a function of U, but GGA+U results are systematically smaller by a constant difference of ∼125 kJ/mol. These features can be rationalized from the viewpoint of chemical bonding. Pure LDA (i.e., U = 0) dramatically favors the LS state characterized by the fully occupied t_{2g} (bonding) orbitals and strong M−L bonds. This tendency along with the underestimation of the M−L bond lengths can be attributed to two drawbacks of LDA:[29] one is the local formulation based on the uniform electron gas, which poorly describes coordination bonds, and the other is the SIE that causes artificial delocalization. The U term tackles the on-site Coulomb interaction to eliminate the severe SIE among localized d-electrons.[39] By increasing U, a large portion or the whole part of the artificial delocalization contribution can be removed from the real hybridization responsible for the M−L bonding. As shown in the inset of Figure 2, the local spin density projected on the iron center increases as a function of U, indicating enhanced localization of the magnetic orbitals. The latter in turn tends to weaken the M−L bonding and reduce the energy bias for the LS states. When an appropriate U (4.0 eV) is used, LDA+U reproduces experimental geometries (in Table S1, Supporting Information) as well as the SCO behavior of the compound. On the other hand, a too large U (> ∼ 5.0 eV) would bring unphysical localization error and therefore overstabilize the HS state.

In the case of GGA+U, the pure GGA (U = 0) already gives results in a good agreement with experiment. This is likely due to the fact that the first drawback of LDA has been largely overcomed by introducing the gradient correction.[29] It also means that GGA+U is vulnerable to overcorrection. With U = 4.0 eV, indeed GGA+U gives qualitatively wrong ground-state spin (negative ΔE_{H-L}) and significantly overestimated M−L bond lengths. Using a smaller U, GGA+U would also be able to give reasonable results. Lebègue et al.[43] reproduced the experimental adiabatic ΔE_{H-L} of a prototype SCO compound $[Fe(phen)_2(NCS)_2]$ using GGA+U with U = 2.5 eV. For our molecular model system, GGA+U with U = ∼1.0 eV gives ΔE_{H-L} and the

Table 5. $Cu^{II}-Cu^{II}$ Exchange Coupling Constants J (cm^{-1})[a] of the Model Compounds

compound	LDA	LDA+U	GGA	GGA+U	B3LYP	expt	ref
$[Cu_2(bpy)_2(H_2O)_2(C_2O_4)]^{2+}$	−2951	−908	−1765	−464	−634[d]	−382	67
$[Cu_2(petdien)_2(C_2O_4)]^{2+}$	−207	−79	−121	−63	−21[d]	−19	68
$[Cu_2(H_2O)_2(AcO)_4]$	−1374	−433	−863	−230	−429[d]	−286	69
$[Cu_2(dmen)_2(\mu\text{-OMe})(O_2C\text{-}L^b)]^{2+}$	132	36	150	−71	−61[d]	−11	70
$[Cu_2(dpt)_2(O_2C\text{-}L^b)_2]^{2+}$	28	13	20	−5	4[d]	2	71
$[Cu_2(phen)_2(AcO)(\mu\text{−}OH)(\mu\text{−}OH_2)]^{2+}$	408	173	223	84	194[d]	111	72
$[Cu_2(O_2CEt)_2{}^c(\mu\text{−}OH)(dpyam)_2]^{+}$	207	102	117	44	198[e]	24	73
$[Cu_2(O_2CEt)(\mu\text{−}OH)(\mu\text{−}OH_2)(bpy)_2]^{2+}$	341	164	239	90	353[e]	149	74
$[Cu_2(Et_5dien)_2(C_2O_4)]^{2+}$	−1003	−321	−622	−149	−266[f]	−75	75
$[Cu_2(bpm)_2(\mu\text{−}OH)_2]^{2+}$	159	184	115	94	224[f]	114	76
$[Cu_2(DMPTD)(\mu\text{-}N_3)(\mu\text{-Cl})Cl_2]$	−181	101	−4	185	226[f]	168	77

[a] Heisenberg Hamiltonian $\hat{H} = -J\hat{S}_i\cdot\hat{S}_j$, where $J = 2(E_{BS} - E_{HS})$. [b] L=(η^5-C_5H_4)Fe^{II}(η^5-C_5H_5). [c] One of the propionato ligands is in the monatomic bridging mode (μ-OCOEt). [d] Ref 96. [e] Ref 97. [f] Ref 98.

local spin density (see the inset in Figure 2) that are close to those from LDA+U with U = 4.0 eV.

From a physical point of view, the Hubbard U plays a similar role as the weight of the exact (HF) exchange in the hybrid functionals approach in the sense that both can correct the severe SIE among localized d-electrons. The connection between DFT+U and the hybrid functionals approach is clearly demonstrated in the recent work by Tran et al.,[93] in which the hybrid functional is implemented only for strongly correlated electrons in localized d or f states as in DFT+U, and it gives results very similar to those from DFT+U. For SCO compounds, inclusion of the HF exchange stabilizes the HS state, so the accuracy of the hybrid functionals approach for $\Delta E_{H\text{-}L}$ depends on the percentage of the HF exchange. The popular B3LYP including 20% exact exchange fails to predict the correct ground spin states of the SCO compounds,[13,92] while its modified variant, B3LYP*, which reduces the HF percentage to 15%, delivers reasonable $\Delta E_{H\text{-}L}$ values.[94,95]

3.2. Exchange Interactions of Binuclear Copper Complexes. Table 5 shows the calculated exchange interaction constants J of the selected binuclear copper complexes in comparison with the results by B3LYP[96−98] and experiment.[67−77] Neither LDA nor GGA can provide acceptable results since the deviations are far beyond the uncertainty in the experimental data ($\sim$ 10 cm^{-1}). In particular, they even predict the wrong interaction types for some compounds. In contrast, B3LYP generally yields qualitatively correct values, indicating clearly the importance of the HF exchange for the description of the intersite exchange interactions. Consistent with the preceding observation on the relation between the U correction and the HF exchange, LDA+U and GGA+U systematically improve the predictions of LDA and GGA, respectively, and give results that are very similar to those of B3LYP. We note in particular that GGA+U is able to describe magnetic interactions of both AFM and FM dicopper complexes.

In a plane-wave based study, Rivero et al.[44] reported that J in FM complexes could not be properly described by DFT+U, which contradicts the finding in this work. They found that the U correction reduced the overestimated results obtained using both LDA and PW91 by no more than 20% (with U = 6.0 eV), resulting in J still 3−8 times larger than experimental values. A precise explanation for this discrepancy is difficult without more detailed information. Here we give some speculation on the possible causes. The BS state in a FM system is metastable and therefore more difficult to reach than that in the AFM case. To find the metastable BS state, it is necessary to start the calculation from a tailored initial guess and caution is needed to ensure the true BS state is found when the self-consistent field (SCF) iteration converges. This issue has been paid particular attention in our calculations. As far as we know, the DFT+U approach has been widely used to study exchange coupling constants of bulk inorganic magnetic systems, where comparable accuracy has been reached for FM and AFM systems (see, e.g., ref 99). We see no particular reasons that molecular magnetic systems should be different in this aspect.

We use $[Cu_2(bpy)_2(H_2O)_2(\mu\text{-}C_2O_4)]^{2+}$ (bpy = 2, 2′-bipyridyl)[67] as a model system to investigate the effect of U in more detail. Figure 3a shows J from LDA (GGA)+U as a function of U. LDA overestimates the absolute value of J by a factor of 7, and GGA only shows a slight improvement, overestimating the result by more than four times. This is again associated with the unphysical delocalization of magnetic orbitals that can be characterized by the local spin density projected on copper centers (see Figure 3b). In fact, the BS approach to the evaluation of J (eqs 3 and 4) is formulated based on the strict localization limit,[100] which can, however, be partly invalidated by the delocalization error of LDA and GGA. The Hubbard U correction included in LDA (GGA)+U improves the situation by suppressing the delocalization, as indicated by the increase of the local spin density on copper ions (Figure 3b). This is reminiscent of Kahn's valence bond model,[101,102] which goes back to the Heitler−London's view of the chemical bond and formulates the exchange coupling constant in terms of natural magnetic orbitals:[26]

$$J = J_{FM} + J_{AFM} \approx 2K_{ab} + 4h_{ab}S_{ab} \quad (5)$$

where K_{ab}, h_{ab}, and S_{ab} refer to the exchange, one-electron, and overlap integrals in terms of certain fragment orbitals (denoted as a and b), respectively.[26] The constant J is therefore governed by the competition between the two terms: the positive FM part $2K_{ab}$ (denoted as J_{FM}) and the negative AFM part $4h_{ab}S_{ab}$ (denoted as J_{AFM}). Increasing localization of the magnetic orbitals lowers absolute values of both terms, thus in most cases reducing the absolute value of J whatever the interaction type may be.

We can also interpret the effects of the U correction in terms of the error cancellation. According to the BS model, J is obtained

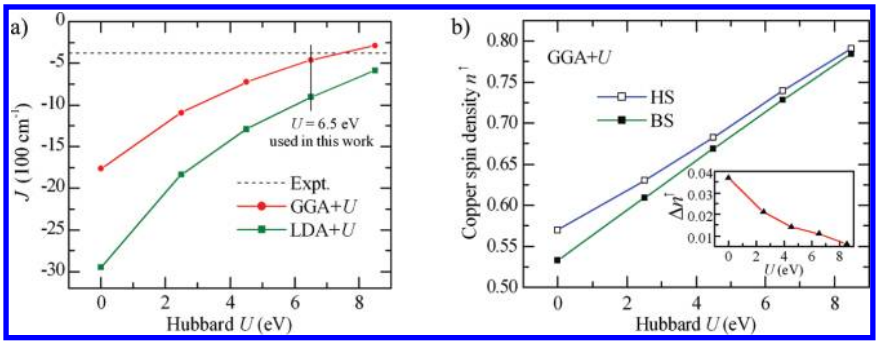

Figure 3. (a) Calculated J [red line, solid circles (●), GGA+U; green line, solid squares (■), LDA+U] under different U values, compared with the experiment (horizontal dash line). The vertical line refers to the value of U used in this work. (b) Spin density $n^{\uparrow}$ (Mulliken population analysis) of one copper center both in HS and BS states obtained using GGA+U for several U values. Inset: spin density difference between HS and BS state $\Delta n^{\uparrow}$ ($n^{\uparrow}_{HS} - n^{\uparrow}_{BS}$) versus U.

from the energy difference between the HS and BS states, which will benefit from extensive cancellation of the errors, including, in particular, the SIE. The extent of the spurious spin delocalization originating from the SIE is slightly different for the HS (↑↑) and the BS (↑↓) states. As shown in Figure 3b, the local spin density on the copper center in the HS state is larger than that in the BS state, implying, in some sense, the incomplete cancellation of the SIE in the two states. The inclusion of U reduces the difference significantly. In the localization limit, the local spin density on Cu(II) in the HS and BS states would become identical, which could be reached by using a very large U. The latter, however, is also unphysical considering that in reality the magnetic moments in these transition-metal complexes are not really local. In other words, the intersite magnetic interaction characterized by the finite J originates from the chemical bonding that relies on the overlap of orbitals on neighboring atoms, i.e., delocalization of electrons. An alternative approach to cancel the SIE is proposed by Rudra et al.[98] in a constrained DFT formalism, in which a binuclear magnetic molecule is divided into two fragments, and J is obtained in terms of eq 4 with the total spin in each fragment fixed to the same value in the HS and BS states. We note, however, that this approach, although physically very sound, might suffer from the drawback that the selection of fragments is not uniquely defined.

4. CONCLUDING REMARKS

In summary, we have investigated the performance of the DFT+U method for the description of both intra-atomic and interatomic spin interaction, the former characterized by the low spin-high spin energy splitting ($\Delta E_{H\text{-}L}$) and the latter by the exchange coupling constant J. We found that LDA+U can reproduce the experimental results in both the electronic and the structural aspects of the SCO compounds. GGA+U approach consistently predicts the exchange coupling constants that are well in agreement with experiment. The comparison with more sophisticated hybrid functionals further confirms the reliability and the applicability of DFT+U approach for the simulation of the SCO systems and the exchange couplings. In addition, we have interpreted the effect of U through the local spin density analysis. The Hubbard U imposes the localization of magnetic orbitals and therefore reduces the overestimated energy splitting between different spin states provided by LDA or GGA.

We close the paper by a few general comments on the DFT+U approach for molecular magnetic systems. As we have shown in this work, the DFT+U approach is quite effective to overcome the delocalization error of LDA or GGA for the description of localized d states in transition-metal complexes. It has the advantage of giving a clear physical picture as well as delivering reasonable accuracy for both intra- and interatomic spin interactions that is comparable to the hybrid functionals approaches. On the other hand, the results from DFT+U depend on U quite strongly. By varying U, electronic states on magnetic centers can change from strongly localized to significantly delocalized. In practice, it is often tempting to use U as an adjustable parameter that makes up for all the possible limitations and uncertainties arising from theoretical models, xc functionals, geometries, and basis sets as well as error bars in experimental data. We adopt a different strategy and choose U based on physical consideration without fitting the target properties under study. In other words, the Hubbard U is introduced mainly to correct the SIE among localized d-electrons. The performance of DFT+U with a particular choice of LDA or GGA then depends not only on the value of U but also on the accuracy of the LDA or GGA for other aspects than the description of localized d states. In this case, it is crucial to establish the overall performance of the DFT+U approach for the properties of interest, based on which reliable prediction can be made, and possible errors can also be estimated. In this work, we have chosen a fixed U for the same transition-metal ion disregarding the different nature of ligands and oxidation states. This is a reasonable first approximation, but a more accurate treatment requires considering the effects of changing chemical environments on the value of U, which can be taken into account by using the constrained DFT approach for the determination of U.[38,86−88]

■ ASSOCIATED CONTENT

Supporting Information. Optimized metal−ligand bond lengths of the iron compounds investigated in this work. This material is available free of charge via the Internet at http://pubs.acs.org.

■ AUTHOR INFORMATION

Corresponding Author
*E-mail: h.jiang@pku.edu.cn.

■ ACKNOWLEDGMENT

We thank Professors Song Gao and Bingwu Wang for helpful discussions. We gratefully thank Prof. Kasper Planeta Jensen,

Technical University of Denmark, and Prof. Francesc Illas, Universitat de Barcelona, for providing us with the crystal data of the model compounds. And we also acknowledge the kind help offered by Dr. Wei Xue and Dr. Jun Jiang. This work is partly supported by the National Natural Science Foundation of China (project no. 20973009).

REFERENCES

(1) Kahn, O. *Molecular Magnetism*; Wiley-VCH: New York, 1993.
(2) Gatteschi, D.; Bogani, L.; Cornia, A.; Mannini, M.; Sorace, L.; Sessoli, R. *Solid State Sci.* **2008**, *10*, 1701.
(3) Sanvito, S.; Rocha, A. R. *J. Comput. Theor. Nanosci.* **2006**, *3*, 624.
(4) Bogani, L.; Wernsdorfer, W. *Nat. Mater.* **2008**, *7*, 179.
(5) Mannini, M.; Pineider, F.; Sainctavit, P.; Danieli, C.; Otero, E.; Sciancalepore, C.; Talarico, A. M.; Arrio, M. A.; Cornia, A.; Gatteschi, D.; Sessoli, R. *Nat. Mater.* **2009**, *8*, 194.
(6) Misiorny, M.; Barnaś, J. *Phys. Rev. B* **2007**, *75*, 134425.
(7) Leuenberger, M. N.; Loss, D. *Nature* **2001**, *410*, 789.
(8) Lehmann, J.; Gaita-Ariño, A.; Coronado, E.; Loss, D. *J. Mater. Chem.* **2009**, *19*, 1672.
(9) Gütlich, P.; Goodwin, H. A. *Top. Curr. Chem.* **2004**, *233*, 1.
(10) Gatteschi, D.; Sessoli, R.; Villain, J. *Molecular Nanomagnets;* Oxford University Press: New York, 2006.
(11) Sato, O.; Tao, J.; Zhang, Y. Z. *Angew. Chem., Int. Ed.* **2007**, *46*, 2152.
(12) Wende, H. *Nat. Mater.* **2009**, *8*, 165.
(13) Paulsen, H.; Trautwein, A. X. *Top. Curr. Chem.* **2004**, *235*, 197.
(14) Cotton, F. A.; Wilkinson, G. *Advanced Inorganic Chemistry*; John Wiley & Sons: Hoboken, NJ, 1988; Chapter 17, pp 625−648.
(15) Sessoli, R.; Gatteschi, D.; Caneschi, A.; Novak, M. A. *Nature* **1993**, *365*, 141.
(16) Van Vleck, J. H. *The Theory of Electric and Magnetic Susceptibilities*; Oxford University Press: Oxford, U.K., 1932.
(17) Neese, F.; Pantazis, D. A. *Faraday Discuss.* **2011**, *148*, 229.
(18) Pierloot, K.; Vancoillie, S. *J. Chem. Phys.* **2008**, *128*, 034104.
(19) Kepenekian, M.; Robert, V.; Guennic, B. L.; Graaf, C. D. *J. Comput. Chem.* **2009**, *30*, 2327.
(20) Vancoillie, S.; Zhao, H.; Radoń, M.; Pierloot, K. *J. Chem. Theory Comput.* **2010**, *6*, 576.
(21) Guennic, B. L.; Amor, N. B.; Maynau, D.; Robert, V. *J. Chem. Theory Comput.* **2009**, *5*, 1506.
(22) Paulovič, J.; Cimpoesu, F.; Ferbinteanu, M.; Hirao, K. *J. Am. Chem. Soc.* **2004**, *126*, 3321.
(23) Perdew, J. P.; Zunger, A. *Phys. Rev. B* **1981**, *23*, 5048.
(24) Harvey, J. N. *Struct. Bonding (Berlin, Ger.)* **2004**, *112*, 151.
(25) Wolny, J. A.; Paulsen, H.; Trautwein, A. X.; Schünemann, V. *Coord. Chem. Rev.* **2009**, *253*, 2423.
(26) Ruiz, E.; Alvarez, S.; Rodriguez-Fortea, A.; Alemany, P.; Pouillon, Y.; Massobrio, C. In *Magnetism: Molecules to Materials*; Miller, J. S., Drillon, M., Ed.; Wiley-VCH: Weinheim, Germany, 2001; Chapter 7, pp 227−279.
(27) Becke, A. D. *J. Chem. Phys.* **1993**, *98*, 1372.
(28) Becke, A. D. *J. Chem. Phys.* **1993**, *98*, 5648.
(29) Koch, W.; Holthausen, M. C. *A Chemist's Guide to Density Functional Theory*; Wiley-VCH: Weinheim, Germany, 2001.
(30) Neese, F. *Coord. Chem. Rev.* **2009**, *253*, 526.
(31) Jensen, K. P.; Cirera, J. *J. Phys. Chem. A* **2009**, *113*, 10033.
(32) Valero, R.; Costa, R.; de, P. R.; Moreira, I.; Truhlar, D. G.; Illas, F. *J. Chem. Phys.* **2008**, *128*, 114103.
(33) Hafner, J. *J. Comput. Chem.* **2008**, *29*, 2044.
(34) Paolo Giannozzi, P.; Baroni, S.; Bonini, N.; Calandra, M.; Car, R.; Cavazzoni, C.; Ceresoli, D.; Chiarotti, G. L.; Cococcioni, M.; Dabo, I.; Corso, A. D.; de Gironcoli, S.; Fabris, S.; Fratesi, G.; Gebauer, R.; Gerstmann, U.; Gougoussis, C.; Kokalj, A.; Lazzeri, M.; Martin-Samos, L.; Marzari, N.; Mauri, F.; Mazzarello, R.; Paolini, S.; Pasquarello, A.; Paulatto, L.; Sbraccia, C.; Scandolo, S.; Sclauzero, G.; Seitsonen, A. P.; Smogunov, A.; Umari, P.; Wentzcovitch, R. M. *J. Phys.: Condens. Matter* **2009**, *21*, 395502.
(35) Hubbard, J. *Proc. R. Soc. A* **1963**, *276*, 238.
(36) Anisimov, V. I.; Zaanen, J.; Andersen, O. K. *Phys. Rev. B* **1991**, *44*, 943.
(37) Dudarev, S. L.; Botton, G. A.; Savrasov, S. Y.; Humphreys, C. J.; Sutton, A. P. *Phys. Rev. B* **1998**, *57*, 1505.
(38) Cococcioni, M.; de Gironcoli, S. *Phys. Rev. B* **2005**, *71*, 035105.
(39) Anisimov, V. I.; Aryasetiawan, F.; Lichtenstein, A. I. *J. Phys.: Condens. Matter* **1997**, *9*, 767.
(40) Karlsson, K.; Aryasetiawan, F.; Jepsen, O. *Phys. Rev. B* **2010**, *81*, 245113.
(41) Boukhvalov, D. W.; Lichtenstein, A. I.; Dobrovitski, V. V.; Katsnelson, M. I.; Harmon, B. N.; Mazurenko, V. V.; Anisimov, V. I. *Phys. Rev. B* **2002**, *65*, 184435.
(42) Scherlis, D. A.; Cococcioni, M.; Sit, P.; Marzari, N. *J. Phys. Chem. B* **2007**, *111*, 7384.
(43) Lebègue, S.; Pillet, S.; Ángyán, J. G. *Phys. Rev. B* **2008**, *78*, 024433.
(44) Rivero, P.; Loschen, C.; de, P. R.; Moreira, I.; Illas, F. *J. Comput. Chem.* **2009**, *30*, 2316.
(45) Gangopadhyay, S.; Masunov, A. E.; Poalelungi, E.; Leuenberger, M. N. *J. Chem. Phys.* **2010**, *132*, 244104.
(46) Sellman, D.; Kunstmann, H.; Moll, M.; Knoch, F. *Inorg. Chim. Acta* **1988**, *154*, 157.
(47) Sellmann, D.; Kunstmann, H.; Knoch, F.; Moll, M. *Inorg. Chem.* **1988**, *27*, 4183.
(48) Sellmann, D.; Hofmann, T.; Knoch, F. *Inorg. Chim. Acta* **1994**, *224*, 61.
(49) Sellmann, D.; Soglowek, W.; Knoch, F.; Ritter, G.; Dengler, J. *Inorg. Chem.* **1992**, *31*, 3711.
(50) Hagen, K. S. *Inorg. Chem.* **2000**, *39*, 5867.
(51) Dose, E. V.; Murphy, K. M. M.; Wilson, L. J. *Inorg. Chem.* **1976**, *15*, 2622.
(52) Sinn, E.; Sim, G.; Dose, E. V.; Tweedle, M. F.; Wilson, L. J. *J. Am. Chem. Soc.* **1978**, *100*, 3375.
(53) Beattie, J. K.; Binstead, R. A.; West, R. J. *J. Am. Chem. Soc.* **1978**, *100*, 3044.
(54) Baker, A. T.; Goodwin, H. A.; Rae, A. D. *Aust. J. Chem.* **1984**, *37*, 443.
(55) Turner, J. W.; Schultz, F. A. *Inorg. Chem.* **1999**, *38*, 358.
(56) Boeyens, J. C. A.; Forbes, A. G. S.; Hancock, R. D.; Wieghardt, K. *Inorg. Chem.* **1985**, *24*, 2926.
(57) Chum, H. L.; Vanin, J. A.; Holanda, M. I. D. *Inorg. Chem.* **1982**, *21*, 1146.
(58) Chernyshov, D.; Hostettler, M.; Tornroos, K. W.; Burgi, H. B. *Angew. Chem., Int. Ed.* **2003**, *42*, 3825.
(59) Jesson, J. P.; Swiatoslaw, T.; Eaton, D. R. *J. Am. Chem. Soc.* **1967**, *89*, 3158.
(60) Oliver, J. D.; Mullica, D. F.; Hutchinson, B. B.; Milligan, W. O. *Inorg. Chem.* **1980**, *19*, 165.
(61) Reeder, K. A.; Dose, E. V.; Wilson, L. J. *Inorg. Chem.* **1978**, *17*, 1071.
(62) Peng, S. M.; Chen, H. F. *Bull. Inst. Chem. Acad. Sin.* **1990**, *37*, 49.
(63) McGarvey, J. J.; Lawthers, I.; Heremans, K.; Toftlund, H. *Inorg. Chem.* **1990**, *29*, 252.
(64) McCusker, J. K.; Rheingold, A. L.; Hendrickson, D. N. *Inorg. Chem.* **1996**, *35*, 2100.
(65) Noodleman, L. *J. Chem. Phys.* **1981**, *74*, 5737.
(66) Ruiz, E.; Cano, J.; Alvarez, S.; Alemany, P. *J. Comput. Chem.* **1999**, *20*, 1391.
(67) Castillo, O.; Muga, I.; Luque, A.; Gutierrez-Zorrilla, J. M.; Sertucha, J.; Vitoria, P.; Roman, P. *Polyhedron* **1999**, *18*, 1235.
(68) Julve, M.; Verdaguer, M.; Gleizes, A.; Philoche-Levisalles, M.; Kahn, O. *Inorg. Chem.* **1984**, *23*, 3808.
(69) de Meester, P.; Fletcher, S. R.; Skapski, A. C. *J. Chem. Soc., Dalton Trans.* **1973**, 2575.
(70) López, C.; Costa, R.; Illas, F.; de Graaf, C.; Turnbull, M. M.; Landee, C. P.; Espinosa, E.; Mata, I.; Molins, E. *Dalton Trans.* **2005**, 2322.

(71) López, C.; Costa, R.; Illas, F.; Molins, E.; Espinosa, E. *Inorg. Chem.* **2000**, *39*, 4560.
(72) Tokii, T.; Hamamura, N.; Nakashima, M.; Muto, Y. *Bull. Chem. Soc. Jpn.* **1992**, *65*, 1214.
(73) Youngme, S.; Chailuecha, C.; van Albada, G. A.; Pakawatchai, C.; Chaichit, N.; Reedijk, J. *Inorg. Chim. Acta* **2005**, *358*, 1068.
(74) Chailuecha, C.; Youngme, S.; Pakawatchai, C.; Chaichit, N.; van Albada, G. A.; Reedijk, J. *Inorg. Chim. Acta* **2006**, *359*, 4168.
(75) Felthouse, T. R.; Laskowski, E. J.; Hendrickson, D. N. *Inorg. Chem.* **1977**, *16*, 1077.
(76) Munno, G. D.; Julve, M.; Lloret, F.; Faus, J.; Verdaguer, M.; Caneschi, A. *Inorg. Chem.* **1995**, *34*, 157.
(77) Tandon, S. S.; Thompson, L. K.; Manuel, M. E.; Bridson, J. N. *Inorg. Chem.* **1994**, *33*, 5555.
(78) Soler, J. M.; Artacho, E.; Gale, J. D.; García, A.; Junquera, J.; Ordejón, P.; Sánchez-Portal, D. *J. Phys.: Condens. Matter* **2002**, *14*, 2745.
(79) Its accuracy and efficiency is mainly controlled by two key parameters: (a) energy shift, defining the cutoff radii of the numerical basis functions used, corresponds to the energy increase due to the confinement of the basis; (b) mesh cutoff controlling the real-space grid, onto which the electron density is to be projected, is equivalent to the plane wave cutoff for the spacing grid. We use 50 meV for the energy shift and 160 Ry for the mesh cutoff.
(80) Artacho, E.; Gale, J. D.; García, A.; Junquera, J.; Martin, R. M.; Ordejón, P.; Sánchez-Portal, D.; Soler, J. M. *SIESTA*, v. LDAU; Universidad Autónoma de Madrid (UAM): Madrid, Spain; http://www.icmab.es/siesta/. (Accessed August 1, 2010).
(81) Martin, R. M. *Electronic Structure: Basic Theory and Practical Methods*: Cambridge University Press: Cambridge, U.K., 2004; Chapter 11, pp 204−231.
(82) Ruiz, E.; Rodríguez-Fortea, A.; Tercero, J.; Cauchy, T.; Massobrio, C. *J. Chem. Phys.* **2005**, *123*, 074102.
(83) Perdew, J. P.; Burke, K.; Ernzerhof, M. *Phys. Rev. Lett.* **1996**, *77*, 3865.
(84) Hüfner, S. *Photoelectron Spectroscopy: Principles and Applications*. 3rd ed. Springer: Berlin, 2003.
(85) Hüfner, S. *Adv. Phys.* **1994**, *43*, 183.
(86) Anisimov, V. I.; Gunnarsson, O. *Phys. Rev. B* **1991**, *43*, 7570.
(87) Nakamura, K.; Arita, R.; Yoshimoto, Y.; Tsuneyuki, S. *Phys. Rev. B* **2006**, *74*, 235113.
(88) Jiang, H.; Gomez-Abal, R. I.; Rinke, P.; Scheffler, M. *Phys. Rev. B* **2010**, *82*, 045108.
(89) Liechtenstein, A. I.; Anisimov, V. I.; Zaanen, J. *Phys. Rev. B* **1995**, *52*, R5467.
(90) Gonze, X. *ABINIT*; Université catholique de Louvain: Louvain-la-Neuve, BELGIUM; http://www.abinit.org/. (Accessed July 1, 2010).
(91) Frisch, M. J.; Trucks, G. W.; Schlegel, H. B.; Scuseria, G. E.; Robb, M. A.; Cheeseman, J. R.; Scalmani, G.; Barone, V.; Mennucci, B.; Petersson, G. A.; Nakatsuji, H.; Caricato, M.; Li, X.; Hratchian, H. P.; Izmaylov, A. F.; Bloino, J.; Zheng, G.; Sonnenberg, J. L.; Hada, M.; Ehara, M.; Toyota, K.; Fukuda, R.; Hasegawa, J.; Ishida, M.; Nakajima, T.; Honda, Y.; Kitao, O.; Nakai, H.; Vreven, T.; Montgomery, J. A., Jr.; Peralta, J. E.; Ogliaro, F.; Bearpark, M.; Heyd, J. J.; Brothers, E.; Kudin, K. N.; Staroverov, V. N.; Kobayashi, R.; Normand, J.; Raghavachari, K.; Rendell, A.; Burant, J. C.; Iyengar, S. S.; Tomasi, J.; Cossi, M.; Rega, N.; Millam, J. M.; Klene, M.; Knox, J. E.; Cross, J. B.; Bakken, V.; Adamo, C.; Jaramillo, J.; Gomperts, R.; Stratmann, R. E.; Yazyev, O.; Austin, A. J.; Cammi, R.; Pomelli, C.; Ochterski, J. W.; Martin, R. L.; Morokuma, K.; Zakrzewski, V. G.; Voth, G. A.; Salvador, P.; Dannenberg, J. J.; Dapprich, S.; Daniels, A. D.; Farkas, O.; Foresman, J. B.; Ortiz, J. V.; Cioslowski, J.; Fox, D. J. *Gaussian 09*, revision A. 01; Gaussian, Inc.: Wallingford, CT, 2009.
(92) Ye, S.; Neese, F. *Inorg. Chem.* **2010**, *49*, 772.
(93) Tran, F.; Blaha, P.; Schwarz, K.; Novák, P. *Phys. Rev. B* **2006**, *74*, 155108.
(94) Shiota, Y.; Sato, D.; Juhász, G.; Yoshizawa, K. *J. Phys. Chem. A* **2010**, *114*, 5862.
(95) Conradie, J.; Ghosh, A. *J. Phys. Chem. B* **2007**, *111*, 12621.
(96) de, P. R.; Moreira, I.; Costa, R.; Filatov, M.; Illas, F. *J. Chem. Theory Comput.* **2007**, *3*, 764.
(97) Costa, R.; de, P. R.; Moreira, I.; Youngme, S.; Siriwong, K.; Wannarit, N.; Illas, F. *Inorg. Chem.* **2010**, *49*, 285.
(98) Rudra, I.; Wu, Q.; Voorhis, T. V. *J. Chem. Phys.* **2006**, *124*, 024103.
(99) Larson, P.; Lambrecht, W. R. L. *J. Phys.: Condens. Matter* **2006**, *18*, 11333.
(100) Caballol, R.; Castell, O.; Illas, F.; de, P. R.; Moreira, I.; Malrieu, J. P. *J. Phys. Chem. A* **1997**, *101*, 7860.
(101) Girerd, J. J.; Journaux, Y.; Kahn, O. *Chem. Phys. Lett.* **1981**, *82*, 534.
(102) Kahn, O. *Inorg. Chim. Acta* **1982**, *62*, 3.